Title

Relationship between mutant Cu/Zn superoxide dismutase 1 maturation and inclusion formation in cell models

Journal

Journal of Neurochemistry, 140(1)

ISSN

0022-3042

Authors

Ayers, Jacob I
McMahon, Benjamin
Gill, Sabrina
et al.

Publication Date

2017

DOI

10.1111/jnc.13864

Peer reviewed

HHS Public Access

Author manuscript

J Neurochem. Author manuscript; available in PMC 2018 January 01.

Published in final edited form as:

J Neurochem. 2017 January ; 140(1): 140–150. doi:10.1111/jnc.13864.

Relationship between mutant SOD1 maturation and inclusion formation in cell models

Jacob I. Ayers[1,*], **Benjamin McMahon**[1,*], **Sabrina Gill**[1,*], **Herman L. Lelie**[2,*], **Susan Fromholt**[1,*], **Hilda Brown**[1], **Joan Selverstone Valentine**[2], **Julian P. Whitelegge**[3], and **David R. Borchelt**[1,†]

[1]Department of Neuroscience, Center for Translational Research in Neurodegenerative Disease, McKnight Brain Institute, University of Florida, Gainesville, Florida 32610

[2]Department of Chemistry and Biochemistry, UCLA, Los Angeles, California 90095

[3]The Pasarow Mass Spectrometry Laboratory, NPI-Semel Institute, David Geffen School of Medicine, UCLA, Los Angeles, California 90024

Abstract

A common property of Cu/Zn superoxide dismutase 1 (SOD1), harboring mutations associated with amyotrophic lateral sclerosis (ALS), is a high propensity to misfold and form abnormal aggregates. The aggregation of mutant SOD1 has been demonstrated in vitro, with purified proteins, in mouse models, in human tissues, and in cultured cell models. *In vitro* translation studies have determined that SOD1 with ALS mutations is slower to mature, and thus perhaps vulnerable to off-pathway folding that could generate aggregates. The aggregation of mutant SOD1 in living cells can be monitored by tagging the protein with fluorescent fluorophores. In the present study, we have taken advantage of the Dendra2 fluorophore technology in which excitation can be used to switch the output color from green to red, thereby clearly creating a time-stamp that distinguishes pre-existing and newly made proteins. In cells that transiently over-express the Ala 4 to Val variant of SOD1-Dendra2, we observed that newly made mutant SOD1 was rapidly captured by pathologic intracellular inclusions. In cell models of mutant SOD1 aggregation over-expressing untagged A4V-SOD1, we observed that immature forms of the protein, lacking a Cu co-factor and a normal intramolecular disulfide, persist for extended periods. Our findings fit with a model in which immature forms of mutant A4V-SOD1, including newly-made protein, are prone to misfolding and aggregation.

†To whom correspondence should be addressed: David Borchelt, Department of Neuroscience/CTRND, Box 100159, University of Florida, Gainesville, FL 32610, USA, Tel.: (352) 273-9664; drb1@ufl.edu.
*These authors contributed equally to this paper.

The authors declare that they have no competing interests.

Supporting information

Additional supporting information may be found in the online version of this article at the publisher's web-site:

Figure S1. Representative images of cells that expressed A4V-SOD1:Dendra2 but had not yet formed inclusions by 16 hours post-transfection.

Figure S2. Representative images of cells that already had formed inclusions containing A4V-SOD1:Dendra2 16 hours post-transfection.

Figure S3. Sensitivity of the oxidized and reduced fractions of NP-40 soluble SOD1 to proteolytic digestion.

Figure S4. Sensitivity of NP-40 insoluble SOD1 to proteolytic digestion.

Figure S5. Sensitivity of the oxidized and reduced fractions of saponin soluble SOD1 to proteolytic digestion.

Figure S6. Metal characterization of soluble SOD1 isolated from HEK293FT cells expressing mutant SOD1.

Graphical abstract

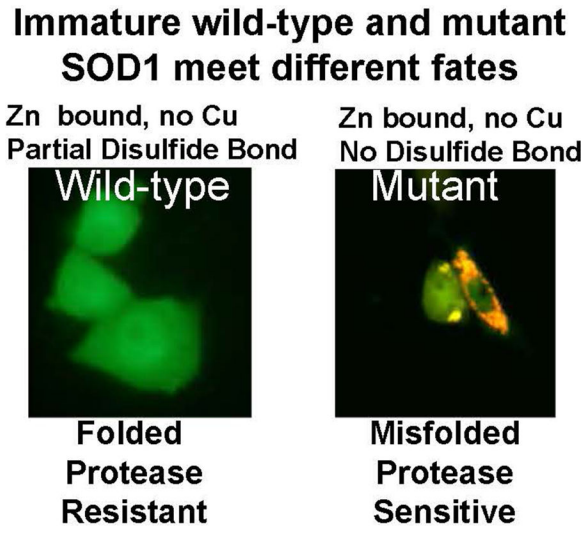

Mutations in Cu/Zn superoxide dismutase 1 (SOD1) may cause amyotrophic lateral sclerosis by misfolding and aggregating. Here, we demonstrate that newly-made mutant SOD1 is rapidly incorporated into growing pathologic intracellular inclusions. Further, we link incomplete post-translational maturation (metal binding and intramolecular disulfide oxidation) of mutant SOD1 to aggregation. These findings suggest that promoting the maturation of mutant SOD1 could produce therapeutic benefits.

Keywords

Amyotrophic Lateral Sclerosis; superoxide dismutase 1; aggregation; oxidation; live-imaging

---

Mutations in Cu/Zn superoxide dismutase 1 (SOD1) cause a familial form of amyotrophic lateral sclerosis that is clinically identical to the more common sporadic form of the disease (Ravits *et al.* 2013; Ravits and La Spada 2009). To date, over 160 different mutations in this enzyme have been reported in ALS patients {http://alsod.iop.kcl.ac.uk/Als/Index.aspx}. Some of these 160 mutations are isolated, apparently *de novo*, mutations without family history, and in these cases establishing these mutations as causal is difficult. Still, there are a large number of mutations that occur in a sufficient frequency in families to establish causality. The most studied SOD1 mutations are those that show clear family history, and these mutations produce differing effects on enzymatic activity and protein stability, with some mutants possessing little or no activity while others retain significant specific activity (Borchelt *et al.* 1994; Hayward *et al.* 2002; Rodriguez *et al.* 2002). Our laboratory has studied more than 40 different ALS variants of SOD1 in cell over-expression models and found that all exhibit an increased propensity to misfold and form abnormal detergent insoluble aggregates (Prudencio *et al.* 2009). *In vitro*, wild-type (WT) human SOD1 can be induced to form fibrillar aggregates (Chattopadhyay *et al.* 2008; Chattopadhyay *et al.* 2015). WT SOD1 also aggregates when highly over-expressed in transgenic mice (Graffmo *et al.* 2013). However, in cultured cell models, WT SOD1 has been much more resistant to aggregation than mutant SOD1 (Prudencio and Borchelt 2011). A pathologic feature of

SOD1-linked fALS that is commonly found is the accumulation of SOD1 immuno-reactive inclusions in surviving spinal motor neurons (Jonsson *et al.* 2008; Sasaki *et al.* 1998; Shaw *et al.* 1997; Shibata *et al.* 1996).

The role of SOD1 aggregation in the pathogenesis of disease is not entirely clear. In the G37R, G93A, H46R/H48Q, and L126Z mouse models our laboratory has shown that large sedimentable, detergent-insoluble, aggregates accumulate to the highest levels as symptoms emerge (Karch *et al.* 2009; Wang *et al.* 2005). Additionally, in transgenic mice that express the ALS variant G85R-SOD1 fused to yellow fluorescent protein (G85R-SOD1:YFP), inclusion-like structures are seen only in mice that are symptomatic and become abundant in motor neuron cell bodies as the mice reach endstage paralysis (Wang *et al.* 2009). More recently, studies of prion-like transmission of motor neuron disease in mice that express G85R-SOD1:YFP have shown that mutant SOD1 inclusion pathology begins to become abundant in motor neurons just as motor deficits begin to appear (Ayers *et al.* 2016). A similar timing of mutant SOD1 aggregation was reported in prion-like transmission studies with mice that express untagged G85R-SOD1 (Bidhendi *et al.* 2016). The timelines for the formation of similar aggregate structures in SOD1-ALS patients is unknown, but SOD1 antibody immunoreactive inclusions and detergent-insoluble aggregates of mutant SOD1 have been described in ALS patient spinal cords (Jonsson *et al.* 2008; Kerman *et al.* 2010; Shibata *et al.* 1994; Watanabe *et al.* 2001).

The normal structure of the 153 amino acid Cu/Zn SOD1 protein is a homodimeric enzyme that matures to native quaternary structure through post-translational modification (Fridovich 1974). These modifications include the formation of a single intra-subunit disulfide bond between residues 57 and 146 of the protein, and the binding of Zn and Cu ions (Ogihara *et al.* 1996; Parge *et al.* 1992). The order in which these modifications are acquired is not completely understood. When expressed and isolated from yeast, human SOD1 encoding a mutation at cysteine 57 (C57S), which abrogates the formation of the normal disulfide bond, purifies with 4 equivalents of Zn per dimer (Sea *et al.* 2015). Crystal structures of this experimental variant show that it achieves a high degree of native dimeric structure (Sea *et al.* 2015). Thus, it seems likely that the binding of Zn is the earliest post-translational event, and that such binding is sufficient to stabilize the structure of individual SOD1 subunits to a level that allows the formation of normal quaternary structure. Further studies of the C57S variant indicate that it is capable of binding Cu in the normal Cu-site, but for WT human SOD1 there is evidence that the disulfide must be reduced in order for Cu to be loaded into the Cu-site (Furukawa *et al.* 2004; Sea *et al.* 2015). Although the binding of Cu certainly contributes to the stability of SOD1, the binding of Zn could be viewed as an earlier and more critical event (Bruns and Kopito 2007). The acquisition of post-translational modifications and assembly into homodimers imparts tremendous stability to WT SOD1 such that it resists proteolytic digestion at concentrations up to 1 mg/ml for 30 min at 37°C (Ratovitski *et al.* 1999). Studies of WT SOD1 maturation in vitro have demonstrated that nascent SOD1 rapidly forms a monomeric intermediate that is resistant to low levels of proteinase (10 μg/ml) but susceptible to higher levels (1 mg/ml), with resistance to the higher levels of proteinase being acquired post-translationally (t1/2 ~19 minutes) (Bruns and Kopito 2007). The binding of Zn is required to achieve the more protease resistant conformation, and the kinetics of intra-subunit disulfide bond formation, and dimerization,

follow closely the kinetics of acquiring high protease K resistance (Bruns and Kopito 2007). All of these data present a picture of SOD1 maturation that suggests that one could expect that any given molecule of nascent WT SOD1 should mature into a fully metallated dimeric enzyme in a period of ~60 minutes.

The effect of fALS mutations in SOD1 on the kinetics of maturation varies to some extent, but in general the effect is to slow the rate of maturation (Bruns and Kopito 2007). ALS-mutations in residues involved in the binding of Cu (H46R and H48Q) slow the rate of dimerization and intramolecular disulfide bond oxidation, but do not prevent these post-translational events (Bruns and Kopito 2007). ALS-mutations in the cysteine residues that produce the intramolecular disulfide bond (C57S and C146R) prevent this modification from occurring, and predictably slow maturation. Interestingly, 50% of the C146R-SOD1 can acquire high resistance to proteinase (Bruns and Kopito 2007). Collectively, these data indicate the post-translational modification of SOD1 influences the rate of maturation, but inherent attributes of the SOD1 sequence largely dictate whether the protein will ultimately fold to acquire native conformation.

The relationship between the maturation of mutant SOD1 and the appearance of misfolded aggregates of these proteins is of interest because understanding this relationship may have implications for pharmacologic intervention to prevent aggregation. Given the effects of ALS mutations on the maturation of SOD1, it is possible that the misfolded forms of the protein may represent species of SOD1 that stray from the normal maturation pathway very early in its biogenesis. However, such a scenario does not fit well with the natural history of the disease in which symptoms and SOD1 aggregates appear months (in mice) or decades (in humans) after birth. From a thermodynamic perspective, it is somewhat easier to imagine that nascent SOD1 might be most prone to fold off-pathway and eventually aggregate. However, another scenario could postulate that SOD1 proteins that have aged and acquired damage might be the source of misfolded protein. In a previous study of SOD1 half-life in vivo, Borchelt and colleagues determined that SOD1, including mutant SOD1, is axonally transported in the slow component in the motor neurons of mice (Borchelt *et al.* 1998). Given the long interval required for transport in the slow component (months), motor neurons would be expected to have a tremendous burden of “older” mutant SOD1. Thus, there are two equally compelling sources of mutant SOD1 in motor neurons *in vivo* that could produce misfolded aggregates.

The aggregation of SOD1 in living cells can be monitored by tagging the protein with fluorescent fluorophores, such as yellow fluorescent protein (Prudencio *et al.* 2010). A study of SOD1 kinetics of aggregation by live cell imaging reported that the G93A variant of human SOD1 converts from a diffuse distribution (soluble), to a punctate distribution (insoluble inclusion) about 120 minutes after cells are treated with a proteasome inhibitor to induce aggregation (Kim *et al.* 2014). Relatively large inclusions form rapidly, over 40 minutes, suggesting that the pool of pre-existing SOD1 is captured into the aggregates. Fluorescence resonance imaging by this same group suggested that the source of the misfolded SOD1 was likely monomeric. In the present study, we have taken advantage of the Dendra2 fluorophore technology in which excitation can be used to switch the output color from green to red, thereby clearly marking pre-existing protein in a live cell (Gurskaya *et al.*

2006). We have used this technique, in cells that transiently express the A4V variant of SOD1 and spontaneously produce intracellular inclusions. We determine that newly made SOD1 is a significant driving force in generating aggregates, but older protein can also be drawn into inclusions once the process has begun. Our findings may have implications for therapies that target SOD1 expression as a therapeutic approach. Older, long-lasting pools of mutant A4V-SOD1 may represent a persistent reservoir of protein that can sustain the production of toxic misfolded SOD1 within cells well after production of new protein has been diminished by gene-silencing therapies.

Methods

SOD1 expression constructs

SOD1 expression plasmids, using the pEF.Bos vector (Mizushima and Nagata 1990) for WT, A4V, G85R, D101G, D101N, and G37R human SOD1 cDNA have been previously described (Ayers *et al.* 2014; Borchelt *et al.* 1994; Prudencio *et al.* 2009). To visualize the aggregation of mutant SOD1, we created a fusion construct of WT and A4V human SOD1 cDNA with the Dendra2 fluorophore (Clontech Laboratories, Mountain View, CA, USA). This construct is similar to SOD1 fusions to yellow fluorescent protein that we have previously described (Prudencio *et al.* 2010; Qualls *et al.* 2013a; Qualls *et al.* 2013b; Roberts *et al.* 2012). The fusion construct of WT-SOD1:Dendra2 and A4V-SOD1:Dendra2 was generated by amplifying the Dendra2 cDNA using oligonucleotides that modified the 5' sequence of Dendra2 to remove the start codon and align the coding frame to be in-frame with SOD1.The construct was produced by excising the YFP fluorophore of pEF.Bos vectors encoding WT-SOD1:YFP and A4V-SOD1:YFP (Prudencio *et al.* 2010) and inserting the Dendra2 cDNA amplicon, using the Infusion cloning kit (Clontech Laboratories). The final construct was sequenced in its entirety to confirm the presence of the A4V mutation, and that the Dendra2 was fused in-frame with no unintended mutations. All recombinant DNA work was approved by the University of Florida Division of Environmental Health & Safety. No live animals were used in this study.

Time Lapse Imaging and Analysis

CHO cells were plated in a 35 mm glass-bottom dish. The cells were washed with DPBS and subsequently transfected with SOD1 A4V-Dendra2 DNA (2 μg) and Lipofectamine 2000 (5 μl) (Invitrogen, Carlsbad, CA, USA), for 24 hours at 37°C with 5% CO_2. The transfection was followed by the addition of complete media (DMEM with 10% horse serum and 2 mM L-glutamine) to the cells. The cells were transferred to a live-scope imager (Nikon Ti-E Inverted Live Cell Imaging System, Tokyo, Japan) at 16 hours post-transfection. After the first time point (T0) image, the cells were flashed for 30 seconds with blue light (405nm) at 50% maximum fluorescence intensity to photo convert the green fluorophore to red. The normalized excitation before and after photoactivation switched from wavelengths of 490 to 553nm and 507 to 573nm for green and red protein, respectively. Images were taken at T0 pre and post-flash over a span of 23 hours at an interval of 15 minutes using the NIS-Elements Image Capture and Analysis Software.

Tissue Culture Transfection

For biochemical studies of SOD1 disulfide bond formation, protease sensitivity, and metal content, the SOD1 constructs (4ug) were transfected into HEK293FT cells using Lipofectamine 2000 (Invitrogen, Carlsbad, CA, USA), for 24 or 48 hours, as indicated in the figure legends, at 37°C with 5% CO_2. After 3–5 hours, complete media (DMEM with 10% horse serum and 2 mM L-glutamine) was added to the cells. The cells were then harvested as described below for the various analyses.

Detergent extraction and trypsin digestion of SOD1 for disulfide bond analysis

The methodology used for determining the detergent solubility of mutant SOD1 and for determining sensitivity to proteolytic digestion have been previously described (Ayers *et al.* 2014). Briefly, after a 24-hour transfection, cells were scraped from the dish in DPBS and washed 3 times in DPBS. After the final wash, cells were lysed by sonication three times for 10 seconds each in 1X TEN buffer containing 1% NP-40, 200 mM iodoacetamide, and 1:100 v/v protease inhibitor cocktail (in experiments involving trypsin digestion, the protease inhibitor cocktail was omitted from all buffers). The lysate was then centrifuged at >100,000 × g for 5 min in an AirFuge to produce supernatant 1 (S1) and pellet (P1) fractions. The S1 fractions were put on ice, and the P1 fractions were washed with the same extraction buffer, sonicated three times for 10 seconds each, and centrifuged at >100,000 × g for 5 min. The supernatant was discarded and the remaining pellet (P2) was resuspended by pulsed sonication in 1X TEN buffer containing 0.5% NP-40, 100 mM iodoacetamide, and protease inhibitors. The protein concentrations of the S1 and P2 fractions were then determined by BCA assay (Pierce Biotechnology, Rockford, IL, USA).

To assess sensitivity to proteolysis, 5 μg of protein in the S1 fraction and 20 μg of protein in the P2 fraction were incubated with trypsin at final concentrations of 0, 10, and 100 μg/ml for 30 minutes at 37°C. Digestions were stopped by the addition of Laemmli sample buffer and immediately boiling the sample at 100°C.

Immunoblot analyses

The methodology for immunoblot analyses has been previously described (Ayers *et al.* 2014). Briefly, 5 μg of protein from the S1 fractions and 20 μg of protein from the P2 fractions were analyzed by SDS-PAGE in 18% Tris-Glycine gels (Invitrogen, Carlsbad, CA, USA). For denaturing/reducing gels, the samples were boiled for 5 minutes in Laemmli sample buffer with β-mercaptoethanol (βME). For non-reducing gels, the βME was omitted from the sample buffer. For non-reducing SDS-PAGE, an in-gel reduction was accomplished by incubating gels in transfer buffer with 2% βME for 10 minutes prior to transferring to nitrocellulose membrane. The immunoblots were probed with two different rabbit polyclonal antibodies, one designated as m/hSOD antibody (Borchelt *et al.* 1994) or one designated as hSOD antibody (Bruijn *et al.* 1998). Primary antibodies were revealed with goat anti-rabbit secondary antibody at 1:5000 (KPL, Gaithersburg, MD, USA) and chemi-luminescence reagents (Thermo Scientific Inc., Rockford, IL, USA), using a Fujifilm imaging system (FUJIFILM Life Science, Stamford, CT, USA). The aggregation propensity was assessed by comparing the ratio of immunoreactive SOD1 bands in the P2 versus S1 fractions as previously described (Prudencio *et al.* 2009).

SOD1 metal-binding characterization

The level of Cu and Zn bound to soluble SOD1 isolated from cultured cells, which had been transfected for 24 hours, was determined using methods previously described (Ayers *et al.* 2014; Lelie *et al.* 2011). The method involved a combination of size exclusion chromatography coupled directly to ICP-MS where Cu, Zn, manganese, and iron concentrations were then measured in real-time allowing for accurate Cu and Zn concentration from the SOD1 peak. SOD1 metallation was determined by dividing SOD1 metal concentration by the SOD1 protein concentration.

Statistical analyses

All statistical analyses were conducted using in GraphPad PRISM 5.01 Software (La Jolla, CA), with the tests used indicated in figure legends. In the live-imaging studies, aggregation propensity was assessed by statistical analysis of the ratio of red to green SOD1-Dendra2 protein in inclusions at each time point.

Results

To visualize the aggregation of A4V-SOD1 in living cells, we constructed fusion proteins of human A4V-SOD1 with the fluorophore Dendra2. We have previously demonstrated that ALS mutant SOD1 tagged with YFP (SOD1:YFP), including the A4V variant, forms cytoplasmic inclusions when expressed in cultured cells, whereas WT-SOD1:YFP does not (Prudencio *et al.* 2010; Prudencio and Borchelt 2011; Qualls *et al.* 2013a; Qualls *et al.* 2013b; Roberts *et al.* 2012). Similarly WT SOD1 tagged with green fluorescent protein does not readily form inclusions when expressed in cultured cells and is fully active (Stevens *et al.* 2010). In most of our prior studies of mutant SOD1 aggregation, we have used the human HEK293 cell model because it allows for the high levels of expression that are required to produce aggregation in the time frame of a typical cell culture experiment. In the present study, however, we found the HEK293 cell model to be problematic for live cell imaging due to cell rounding, which produces shifts in the focal plane and obscures visualization of the cytoplasmic inclusions. In identifying a replacement, we observed that CHO cells were superior in live cell imaging morphology. In previous work, we have demonstrated that fusions of mutant SOD1:YFP proteins readily produce inclusion structures in CHO cells, whereas WT-SOD1:YFP do not (Roberts *et al.* 2012). To confirm that the Dendra2 fluorophore was not inducing SOD1 aggregation, we generated a WT-SOD1 fused to Dendra2 and expressed it in CHO cells for 48 hours. No inclusions were observed in the cells expressing WT-SOD1:Dendra2, whereas abundant inclusions were produced in cells transiently transfected with the SOD1 mutant A4V fused to Dendra2 (A4V-SOD1:Dendra2) (Fig 1).

The basic paradigm used here was to transfect cells, then wait 16 hours before exposing to a blue light flash to photo-convert the emission of the fluorophore from green to red. By this method, any A4V-SOD1:Dendra2 protein made over the initial 16 hours would emit in the red spectrum and any newly-made protein would emit in the green spectrum. The flashed cells were then incubated for an additional 22 hours in a live imaging microscope. In analyzing the resulting video images, we focused our attention on two types of cells. One

focus was on cells that contained diffusely distributed A4V-SOD1:Dendra2, and the other focus was on cells that had already developed inclusions by 16 hours post-transfection.

In a subset of cells that demonstrated only diffusely distributed A4V-SOD1-Dendra2 (green) at pre-flash, inclusions could be detected forming at about 12 hours post-flash (Fig. 2, Fig. S1). In these cells, we observed a fairly similar intensity of fluorescence in both the green (newly-made) and red (older protein) channels. As the inclusions grew in size over an additional 6 hours (18 hours post-flash), there seemed to be a relatively equivalent increase in both the green and red emitting forms of A4V-SOD1:Dendra2 in the inclusions (Fig. 2, Table 1, Fig. S2). We observed that all of the cells that gained red fluorescent inclusions over time also gained newly-made, green inclusions (Table 1). In cells in which inclusions were evident prior to the flash, we observed a relatively rapid capture of newly-made A4V-SOD1:Dendra2 (green) protein by the pre-existing inclusions (red) (Fig. 3, Table 1, Fig. S2). This phenomenon appeared in almost all cells that had pre-existing inclusions at 0 hours (Table 1). Collectively, these observations suggest that newly-made A4V-SOD1:Dendra2 protein is highly vulnerable to capture in growing aggregates, but much older forms of this protein can also be captured. In this model, it seems that both the newly-made and older, presumably more mature, pools of A4V-SOD1:Dendra2 are similarly vulnerable to capture into growing inclusions.

To more fully understand the dynamics of WT and mutant A4V-SOD1 maturation in cultured cell models, we examined the oxidation state, protease sensitivity, and metalation of expressed protein. For this component of the study, we turned back to the HEK293FT cell model that has been used extensively to study the aggregation of untagged mutant SOD1 (Karch and Borchelt 2010; Prudencio *et al.* 2009; Wang *et al.* 2003). Prior studies by Zetterstrom and colleagues demonstrated that SOD1 proteins lacking the normal intramolecular disulfide bond can be discriminated from proteins with the correct linkage by non-reducing, denaturing, SDS-PAGE (Zetterstrom *et al.* 2007). SOD1 with a normal intramolecular disulfide (oxidized – O) migrates slightly faster in these gels than the reduced protein due to differences in the shape of the molecules. As previously reported (Ayers *et al.* 2014), when over-expressed, WT SOD1 is slow to acquire the normal intramolecular disulfide bond, but eventually slightly more than 50% of the protein is correctly oxidized by 48 hrs post-transfection (Fig. 4; Supplemental Fig. S3). By contrast, >80% of the A4V variant protein never acquires an intramolecular disulfide bond.

We next examined maturation of WT and A4V SOD1 into protease-resistant conformations. In previous work, we have demonstrated that natively folded WT SOD1 is extremely resistant to proteolytic degradation (Ratovitski *et al.* 1999). To examine the protease sensitivity of mutant SOD1, we have used a strategy in which soluble and insoluble forms of the protein are analyzed separately by first fractionating cell lysates by detergent extraction and centrifugation (Wang *et al.* 2003). At 48 hours post-transfection, both oxidized and reduced forms of WT SOD1 are detected in NP40 soluble fractions [Fig. 5A; Fig. S3; also see (Ayers *et al.* 2014)]. Both of these forms of WT protein are resistant to proteolytic digestion (Fig. 5A and B; Fig. S3), with the reduced form being somewhat more sensitive (Fig. 5B). The vast majority of NP-40 soluble A4V SOD1 in these cells is reduced, and this reduced form of the protein is highly sensitive to protease digestion (Fig. 5A and C; Fig.

S3). At the exposure used in these immunoblots, the endogenous SOD1 in these cells cannot be seen (see Fig. S3) and thus the faint band of reactivity that migrates as oxidized protein is A4V mutant SOD1 that is largely resistant to protease attack (Fig. 5A and C). Notably, there is also a minor fraction of reduced A4V that is resistant to digestion (Fig. 5A). Overall, however, in buffers containing NP40, the A4V variant of SOD1 is much less resistant to proteolytic digestion than the WT variant.

Other ALS variants of SOD1 exhibit similar properties when over-expressed (Fig. S3). NP40 soluble forms of the G85R-SOD1 are likely reduced (difficult to definitively demonstrate by electrophoretic migration), and are highly sensitive to proteolytic digestion. As previously described (Ayers *et al.* 2014), most of the NP40 soluble D101N and D101G variants of SOD1 that are detected in over-expressing cells migrate as reduced protein that is protease sensitive (Fig. S3). The G37R variant contrasts somewhat, as a greater percentage of the reduced form of this variant is resistant to protease digestion (Fig. S3). Still, as a whole, when highly over-expressed, ALS variants of SOD1 are less able to mature into protease-resistant conformations.

Mutant forms of SOD1, including the A4V variant, misfold and aggregate to become insoluble in NP40 (Wang *et al.* 2003). By 48 hours post-transfection, very little of WT SOD1 adopts the NP40-insoluble conformation (Wang *et al.* 2003)(Suppl. Fig. S4A). Similar to the soluble A4V-SOD1, the insoluble forms of this protein are also sensitive to trypsin digestion (Fig. S4). Detergent-insoluble A4V SOD1 is partially resistant to trypsin at 10 μg/ml, but completely degraded at 100 μg/ml. Interestingly, aggregated forms of the mutants examined here (A4V, G37R, G85R, D101N, D101G) show remarkably similar profiles of protease sensitivity (Fig. S4), suggesting the aggregated forms of these mutants may share structural features.

An important point to emphasize in the foregoing studies is that the trypsin digestions were carried out in buffers containing NP40. When we liberate soluble WT and A4V SOD1 by treatment of cells with saponin (Prudencio and Borchelt 2011) and digest the proteins in the buffers containing saponin, then the sensitivity of reduced A4V SOD1 to digestion is less dramatic, although still distinguishable from WT (Fig. S5). Similarly, reduced forms of the G37R variant show less sensitivity to digestion (Fig. S5). Presumably, the difference in degree of sensitivity to digestion in the two experiments is due to effects of NP40 on the accessibility of trypsin cleavage sites in the mutant protein, with the detergent acting to increase accessibility. Notably, reduced forms of other mutants, such as G85R, D101G, and D101N [also see (Ayers *et al.* 2014)] display high sensitivity to protease digestion in buffers containing saponin. These data provide an indication of the influence of detergents on the protease sensitivity of mutant SOD1.

To determine metal content of the proteins in these cells, we isolated the over-expressed SOD1 by HPLC fractionation and then analyzed the SOD1 containing fractions by ICP-MS (Ayers *et al.* 2014). The metal content of A4V-SOD1 isolated from these cells at 24 h post-transfection was similar to that of WT-SOD1 [data for untransfected cells and cells expressing WT SOD1 reproduced from (Ayers *et al.* 2014)]. The level of bound Cu was less than 0.5 equivalents per dimer, with both WT and A4V SOD1 containing about 2

equivalents of Zn per dimer (Fig. 6; Fig. S6). In this over-expression model, the metal content in the A4V variant was similar to that of G37R variant (Fig. S6). By contrast, the G85R, D101G, and D101N variants were all distinguished by low incorporation of both Cu and Zn [Fig. S6; see (Ayers *et al.* 2014)]. Comparing these data to what is observed for endogenous SOD1 in these same cells, it is clear that over-expressed WT or mutant SOD1 did not acquire Cu efficiently, with the incorporation of Zn being more variable between mutants.

Discussion

In cells over-expressing mutant SOD1, we have modeled the spontaneous aggregation of A4V mutant protein, using both visual and biochemical means of assessing aggregation. In our study of SOD1 fused to the Dendra2 fluorescent reporter protein, our primary goal was to determine whether newly synthesized A4V SOD1 was disproportionately prone to aggregation and inclusion formation. As SOD1 matures, it acquires several post-translational modifications that would stabilize structure, including the binding of Cu, Zn, and an intramolecular disulfide bond. Intuitively, it would seem far easier for mutant protein that has failed to mature to be recruited into aggregates than to have a mature protein essentially unfold. Although we find that newly made A4V SOD1 is highly prone to aggregation, we also find that older, pre-existing, mutant SOD1 can be recruited to growing aggregates relatively efficiently. Presumably, older protein, which in this study includes proteins that are 1 to 2 hours old, would be more mature than newly made protein (Bruns and Kopito 2007). Thus, on face value, our data from the SOD1-Dendra2 study would suggest that more mature A4V-SOD1 can be templated to misfold in cells with growing aggregates. Importantly, in all cells producing A4V-SOD1-Dendra2 inclusions, the newly-made protein was invariably recruited to such structures, indicating that once aggregation has initiated, newly-made mutant SOD1 may be highly vulnerable to accretion into growing inclusions. An important feature of the cell models used here to examine the spontaneous aggregation of mutant SOD1 is that the mutant proteins must be highly over expressed. Our biochemical analysis of over-expressed A4V SOD1 indicates that a large portion of the protein in these cells does not acquire two of the structure-stabilizing post-translational modifications (Cu binding and intramolecular disulfide bond formation). Over-expressed A4V SOD1 is generally less well folded, even after 48 hours post-transfection, as indicated by sensitivity to trypsin digestion in non-ionic detergents. It is important to note that when WT SOD1 is over-expressed in the same manner, it too fails to bind Cu, with a large fraction ~50% failing to form the normal disulfide bond. Yet, when expressed to equivalent levels as mutant SOD1, the WT protein does not spontaneously misfold and aggregate. Thus, a lack of post-translational maturation due to over-expression is not necessarily a defining feature that causes aggregation.

Still, our data suggest that one of the reasons that it may be possible to model mutant SOD1 aggregation in over-expressed cells is that a large portion of the over-expressed protein fails to acquire structure stabilizing modifications. All mutants we have examined here, in this paradigm, largely fail to acquire Cu and oxidize the disulfide. In buffers containing NP40, the conformation of the reduced form of expressed mutant SOD1 leaves these proteins more sensitive, to varying degrees, to protease digestion than WT SOD1. Interestingly, although

soluble forms of the mutants we have examined show differing sensitivities to protease digestion, the aggregated forms of these mutants show remarkably similar profiles of protease sensitivity (see Fig. S4), suggesting the aggregated forms of these mutants may share structural features. The collective conclusion from these studies is that in cell culture models in which spontaneous aggregation of mutant SOD1 is observed, the majority of expressed protein has not properly matured. Importantly, we and others have shown that the mutant SOD1 that accumulates as detergent insoluble aggregates in SOD1-ALS mouse models appears to be derived from immature precursors, lacking the normal disulfide bond (Karch and Borchelt 2008; Karch *et al.* 2009; Zetterstrom *et al.* 2007). Studies *in vitro* have similarly shown that intramolecular disulfide bond formation is a key event in controlling the fibrillation of SOD1 (Chattopadhyay *et al.* 2015). The binding of Zn to immature SOD1 has also been shown in influence its aggregation *in vitro*, producing amorphous aggregates rather than fibrillary structures (Leal *et al.* 2015). Notably, our analysis of mutant A4V SOD1 metalation in our cell model indicated that most of the protein possessed 2 Zn per dimer (see Fig. 6). We conclude that if immature forms of mutant SOD1 (particularly disulfide-reduced forms) exist at any level under physiological conditions, then such forms of the protein would be very prone to aggregate. This conclusion implies that small molecules that improve the maturation of mutant SOD1 might reduce the burden of toxic protein and slow the progression of SOD1-linked ALS. One example of such a molecule might be CuATSM, which improves Cu delivery in the G93A-SOD1 mouse model of over-expression and extends life span (Williams *et al.* 2016). Our data also predict that inhibition of mutant SOD1 production in patients by gene-silencing therapies should substantially reduce the burden of misfolded protein aggregates by reducing the pool of immature SOD1 proteins that are highly prone to aggregation.

Supplementary Material

Refer to Web version on PubMed Central for supplementary material.

Acknowledgments

This work was funded by a grant from the National Institutes of Neurological Disease and Stroke (P01 NS049134 – Program Project), by the UCSD/UCLA NIDDK Diabetes Research Center P30 DK063491 (JW), and by the Amyotrophic Lateral Sclerosis Association (fellowship to J.A.).

Abbreviations used

ALS	amyotrophic lateral sclerosis
CHO cells	Chinese Hamster Ovary cells
fALS	familial ALS
HEK293 cells	Human embryonic kidney #293 cells
PBS	phosphate buffered saline
SDS-PAGE	sodium dodecyl sulfate-polyacrylamide gel electrophoresis
SOD1	Cu/Zn superoxide dismutase 1

YFP	yellow fluorescent protein

References

Ayers J, Lelie H, Workman A, Prudencio M, Brown H, Fromholt S, Valentine J, Whitelegge J, Borchelt D. Distinctive features of the D101N and D101G variants of superoxide dismutase 1; two mutations that produce rapidly progressing motor neuron disease. J. Neurochem. 2014; 128:305–314. [PubMed: 24032979]

Ayers JI, Fromholt SE, O'Neal VM, Diamond JH, Borchelt DR. Prion-like propagation of mutant SOD1 misfolding and motor neuron disease spread along neuroanatomical pathways. Acta Neuropathol. 2016; 131:103–114. [PubMed: 26650262]

Bidhendi EE, Bergh J, Zetterstrom P, Andersen PM, Marklund SL, Brannstrom T. Two superoxide dismutase prion strains transmit amyotrophic lateral sclerosis-like disease. J. Clin. Invest. 2016; 126:2249–2253. [PubMed: 27140399]

Borchelt DR, Lee MK, Slunt HS, Guarnieri M, Xu ZS, Wong PC, Brown RH Jr, Price DL, Sisodia SS, Cleveland DW. Superoxide dismutase 1 with mutations linked to familial amyotrophic lateral sclerosis possesses significant activity. Proc. Natl. Acad. Sci. U. S. A. 1994; 91:8292–8296. [PubMed: 8058797]

Borchelt DR, Wong PC, Becher MW, Pardo CA, Lee MK, Xu ZS, Thinakaran G, Jenkins NA, Copeland NG, Sisodia SS, Cleveland DW, Price DL, Hoffman PN. Axonal transport of mutant superoxide dismutase 1 and focal axonal abnormalities in the proximal axons of transgenic mice. Neurobiol. Dis. 1998; 5:27–35. [PubMed: 9702785]

Bruijn LI, Houseweart MK, Kato S, Anderson KL, Anderson SD, Ohama E, Reaume AG, Scott RW, Cleveland DW. Aggregation and motor neuron toxicity of an ALS-linked SOD1 mutant independent from wild-type SOD1. Science. 1998; 281:1851–1854. [PubMed: 9743498]

Bruns CK, Kopito RR. Impaired post-translational folding of familial ALS-linked Cu, Zn superoxide dismutase mutants. EMBO J. 2007; 26:855–866. [PubMed: 17255946]

Chattopadhyay M, Durazo A, Sohn SH, Strong CD, Gralla EB, Whitelegge JP, Valentine JS. Initiation and elongation in fibrillation of ALS-linked superoxide dismutase. Proc. Natl. Acad. Sci. U. S. A. 2008; 105:18663–18668. [PubMed: 19022905]

Chattopadhyay M, Nwadibia E, Strong CD, Gralla EB, Valentine JS, Whitelegge JP. The Disulfide Bond, but Not Zinc or Dimerization, Controls Initiation and Seeded Growth in Amyotrophic Lateral Sclerosis-linked Cu,Zn Superoxide Dismutase (SOD1) Fibrillation. J. Biol. Chem. 2015; 290:30624–30636. [PubMed: 26511321]

Fridovich I. Superoxide dismutases. Adv. Enzymol. Relat. Areas Mol. Biol. 1974; 41:35–97. [PubMed: 4371571]

Furukawa Y, Torres AS, O'Halloran TV. Oxygen-induced maturation of SOD1: a key role for disulfide formation by the copper chaperone CCS. EMBO J. 2004; 23:2872–2881. [PubMed: 15215895]

Graffmo KS, Forsberg K, Bergh J, Birve A, Zetterstrom P, Andersen PM, Marklund SL, Brannstrom T. Expression of wild-type human superoxide dismutase-1 in mice causes amyotrophic lateral sclerosis. Hum. Mol. Genet. 2013; 22:51–60. [PubMed: 23026746]

Gurskaya NG, Verkhusha VV, Shcheglov AS, Staroverov DB, Chepurnykh TV, Fradkov AF, Lukyanov S, Lukyanov KA. Engineering of a monomeric green-to-red photoactivatable fluorescent protein induced by blue light. Nat. Biotechnol. 2006; 24:461–465. [PubMed: 16550175]

Hayward LJ, Rodriguez JA, Kim JW, Tiwari A, Goto JJ, Cabelli DE, Valentine JS, Brown RH Jr. Decreased Metallation and Activity in Subsets of Mutant Superoxide Dismutases Associated with Familial Amyotrophic Lateral Sclerosis. J. Biol. Chem. 2002; 277:15923–15931. [PubMed: 11854284]

Jonsson PA, Bergemalm D, Andersen PM, Gredal O, Brannstrom T, Marklund SL. Inclusions of amyotrophic lateral sclerosis-linked superoxide dismutase in ventral horns, liver, and kidney. Ann. Neurol. 2008; 63:671–675. [PubMed: 18409196]

Karch CM, Borchelt DR. Aggregation modulating elements in mutant human superoxide dismutase 1. Arch. Biochem. Biophys. 2010; 503:175–182. [PubMed: 20682279]

Karch CM, Borchelt DR. A limited role for disulfide cross-linking in the aggregation of mutant SOD1 linked to familial amyotrophic lateral sclerosis. J. Biol. Chem. 2008; 283:13528–13537. [PubMed: 18316367]

Karch CM, Prudencio M, Winkler DD, Hart PJ, Borchelt DR. Role of mutant SOD1 disulfide oxidation and aggregation in the pathogenesis of familial ALS. Proc. Natl. Acad. Sci. U. S. A. 2009; 106:7774–7779. [PubMed: 19416874]

Kerman A, Liu HN, Croul S, Bilbao J, Rogaeva E, Zinman L, Robertson J, Chakrabartty A. Amyotrophic lateral sclerosis is a non-amyloid disease in which extensive misfolding of SOD1 is unique to the familial form. Acta Neuropathol. 2010; 119:335–344. [PubMed: 20111867]

Kim J, Lee H, Lee JH, Kwon DY, Genovesio A, Fenistein D, Ogier A, Brondani V, Grailhe R. Dimerization, oligomerization, and aggregation of human amyotrophic lateral sclerosis copper/zinc superoxide dismutase 1 protein mutant forms in live cells. J. Biol. Chem. 2014; 289:15094–15103. [PubMed: 24692554]

Leal SS, Cristovao JS, Biesemeier A, Cardoso I, Gomes CM. Aberrant zinc binding to immature conformers of metal-free copper-zinc superoxide dismutase triggers amorphous aggregation. Metallomics. 2015; 7:333–346. [PubMed: 25554447]

Lelie HL, Liba A, Bourassa MW, Chattopadhyay M, Chan PK, Gralla EB, Miller LM, Borchelt DR, Valentine JS, Whitelegge JP. Copper and zinc metallation status of copper-zinc superoxide dismutase from amyotrophic lateral sclerosis transgenic mice. J. Biol. Chem. 2011; 286:2795–2806. [PubMed: 21068388]

Mizushima S, Nagata S. pEF-BOS, a powerful mammalian expression vector. Nucleic Acids Res. 1990; 18:5322. [PubMed: 1698283]

Ogihara NL, Parge HE, Hart PJ, Weiss MS, Goto JJ, Crane BR, Tsang J, Slater K, Roe JA, Valentine JS, Eisenberg D, Tainer JA. Unusual trigonal-planar copper configuration revealed in the atomic structure of yeast copper-zinc superoxide dismutase. Biochemistry. 1996; 35:2316–2321. [PubMed: 8652572]

Parge HE, Hallewell RA, Tainer JA. Atomic structures of wild-type and thermostable mutant recombinant human Cu,Zn superoxide dismutase. Proc. Natl. Acad. Sci. U. S. A. 1992; 89:6109–6113. [PubMed: 1463506]

Prudencio M, Borchelt DR. Superoxide dismutase 1 encoding mutations linked to ALS adopts a spectrum of misfolded states. Mol. Neurodegener. 2011; 6:77. [PubMed: 22094223]

Prudencio M, Durazo A, Whitelegge JP, Borchelt DR. An examination of wild-type SOD1 in modulating the toxicity and aggregation of ALS-associated mutant SOD1. Hum. Mol. Genet. 2010; 19:4774–4789. [PubMed: 20871097]

Prudencio M, Hart PJ, Borchelt DR, Andersen PM. Variation in aggregation propensities among ALS-associated variants of SOD1: correlation to human disease. Hum. Mol. Genet. 2009; 18:3217–3226. [PubMed: 19483195]

Qualls DA, Crosby K, Brown H, Borchelt DR. An analysis of interactions between fluorescently-tagged mutant and wild-type SOD1 in intracellular inclusions. PLoS One. 2013a; 8:e83981. [PubMed: 24391857]

Qualls DA, Prudencio M, Roberts BL, Crosby K, Brown H, Borchelt DR. Features of wild-type human SOD1 limit interactions with misfolded aggregates of mouse G86R Sod1. Mol. Neurodegener. 2013b; 8 46-1326-8-46.

Ratovitski T, Corson LB, Strain J, Wong P, Cleveland DW, Culotta VC, Borchelt DR. Variation in the biochemical/biophysical properties of mutant superoxide dismutase 1 enzymes and the rate of disease progression in familial amyotrophic lateral sclerosis kindreds. Hum. Mol. Genet. 1999; 8:1451–1460. [PubMed: 10400992]

Ravits J, Appel S, Baloh RH, Barohn R, Rix BB, Elman L, Floeter MK, Henderson C, Lomen-Hoerth C, Macklis JD, McCluskey L, Mitsumoto H, Przedborski S, Rothstein J, Trojanowski JQ, van dB, Ringel S. Deciphering amyotrophic lateral sclerosis: What phenotype, neuropathology and genetics are telling us about pathogenesis. Amyotroph. Lateral. Scler. Frontotemporal. Degener. 2013; 14(Suppl 1):5–18. [PubMed: 23678876]

Ravits JM, La Spada AR. ALS motor phenotype heterogeneity, focality, and spread: deconstructing motor neuron degeneration. Neurology. 2009; 73:805–811. [PubMed: 19738176]

Roberts BL, Patel K, Brown HH, Borchelt DR. Role of disulfide cross-linking of mutant SOD1 in the formation of inclusion-body-like structures. PLoS One. 2012; 7:e47838. [PubMed: 23118898]

Rodriguez JA, Valentine JS, Eggers DK, Roe JA, Tiwari A, Brown RH Jr, Hayward LJ. Familial Amyotrophic Lateral Sclerosis-associated Mutations Decrease the Thermal Stability of Distinctly Metallated Species of Human Copper/Zinc Superoxide Dismutase. J. Biol. Chem. 2002; 277:15932–15937. [PubMed: 11854285]

Sasaki S, Ohsawa Y, Yamane K, Sakuma H, Shibata N, Nakano R, Kikugawa K, Mizutani T, Tsuji S, Iwata M. Familial amyotrophic lateral sclerosis with widespread vacuolation and hyaline inclusions. Neurology. 1998; 51:871–873. [PubMed: 9748044]

Sea K, Sohn SH, Durazo A, Sheng Y, Shaw BF, Cao X, Taylor AB, Whitson LJ, Holloway SP, Hart PJ, Cabelli DE, Gralla EB, Valentine JS. Insights into the role of the unusual disulfide bond in copper-zinc superoxide dismutase. J. Biol. Chem. 2015; 290:2405–2418. [PubMed: 25433341]

Shaw CE, Enayat ZE, Powell JF, Anderson VE, Radunovic A, al-Sarraj S, Leigh PN. Familial amyotrophic lateral sclerosis. Molecular pathology of a patient with a SOD1 mutation. Neurology. 1997; 49:1612–1616. [PubMed: 9409355]

Shibata N, Hirano A, Kobayashi M, Sasaki S, Kato T, Matsumoto S, Shiozawa Z, Komori T, Ikemoto A, Umahara T. Cu/Zn superoxide dismutase-like immunoreactivity in Lewy body-like inclusions of sporadic amyotrophic lateral sclerosis. Neurosci. Lett. 1994; 179:149–152. [PubMed: 7845611]

Shibata N, Hirano A, Kobayashi M, Siddique T, Deng HX, Hung WY, Kato T, Asayama K. Intense superoxide dismutase-1 immunoreactivity in intracytoplasmic hyaline inclusions of familial amyotrophic lateral sclerosis with posterior column involvement. J. Neuropathol. Exp. Neurol. 1996; 55:481–490. [PubMed: 8786408]

Stevens JC, Chia R, Hendriks WT, Bros-Facer V, van MJ, Martin JE, Jackson GS, Greensmith L, Schiavo G, Fisher EM. Modification of superoxide dismutase 1 (SOD1) properties by a GFP tag--implications for research into amyotrophic lateral sclerosis (ALS). PLoS. ONE. 2010; 5:e9541. [PubMed: 20221404]

Wang J, Farr GW, Zeiss CJ, Rodriguez-Gil DJ, Wilson JH, Furtak K, Rutkowski DT, Kaufman RJ, Ruse CI, Yates JR III, Perrin S, Feany MB, Horwich AL. Progressive aggregation despite chaperone associations of a mutant SOD1-YFP in transgenic mice that develop ALS. Proc. Natl. Acad. Sci. U. S. A. 2009; 106:1392–1397. [PubMed: 19171884]

Wang J, Slunt H, Gonzales V, Fromholt D, Coonfield M, Copeland NG, Jenkins NA, Borchelt DR. Copper-binding-site-null SOD1 causes ALS in transgenic mice: aggregates of non-native SOD1 delineate a common feature. Hum. Mol. Genet. 2003; 12:2753–2764. [PubMed: 12966034]

Wang J, Xu G, Li H, Gonzales V, Fromholt D, Karch C, Copeland NG, Jenkins NA, Borchelt DR. Somatodendritic accumulation of misfolded SOD1-L126Z in motor neurons mediates degeneration: {alpha}B-crystallin modulates aggregation. Hum. Mol. Genet. 2005; 14:2335–2347. [PubMed: 16000321]

Watanabe M, Dykes-Hoberg M, Culotta VC, Price DL, Wong PC, Rothstein JD. Histological Evidence of Protein Aggregation in Mutant SOD1 Transgenic Mice and in Amyotrophic Lateral Sclerosis Neural Tissues. Neurobiol. Dis. 2001; 8:933–941. [PubMed: 11741389]

Williams JR, Trias E, Beilby PR, Lopez NI, Labut EM, Bradford CS, Roberts BR, McAllum EJ, Crouch PJ, Rhoads TW, Pereira C, Son M, Elliott JL, Franco MC, Estevez AG, Barbeito L, Beckman JS. Copper delivery to the CNS by CuATSM effectively treats motor neuron disease in SOD(G93A) mice co-expressing the Copper-Chaperone-for-SOD. Neurobiol. Dis. 2016; 89:1–9. [PubMed: 26826269]

Zetterstrom P, Stewart HG, Bergemalm D, Jonsson PA, Graffmo KS, Andersen PM, Brannstrom T, Oliveberg M, Marklund SL. Soluble misfolded subfractions of mutant superoxide dismutase-1s are enriched in spinal cords throughout life in murine ALS models. Proc. Natl. Acad. Sci. U. S. A. 2007; 104:14157–14162. [PubMed: 17715066]

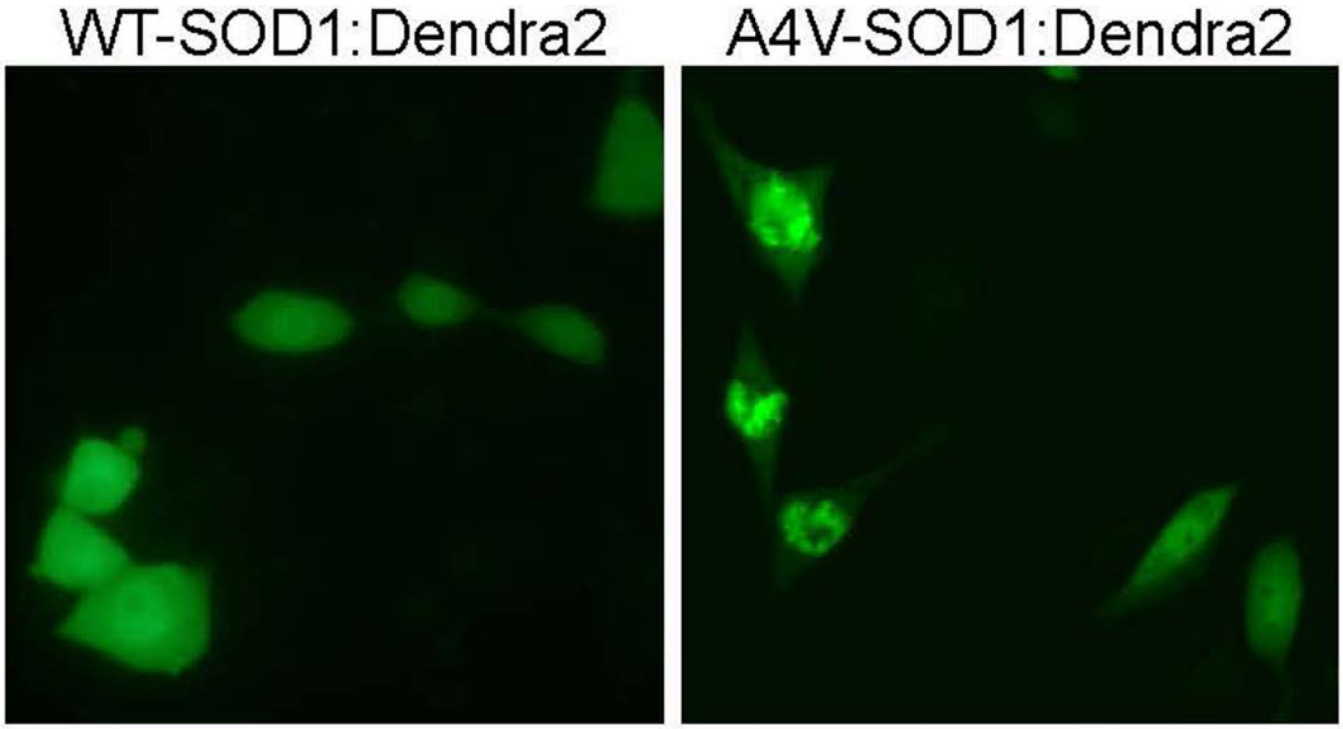

Fig. 1.

Effects of Dendra2 fusion on SOD1 inclusion formation. Representative images of CHO cells at 48 hours following transient transfection with WT-SOD1:Dendra2 or A4V-SOD1:Dendra2.

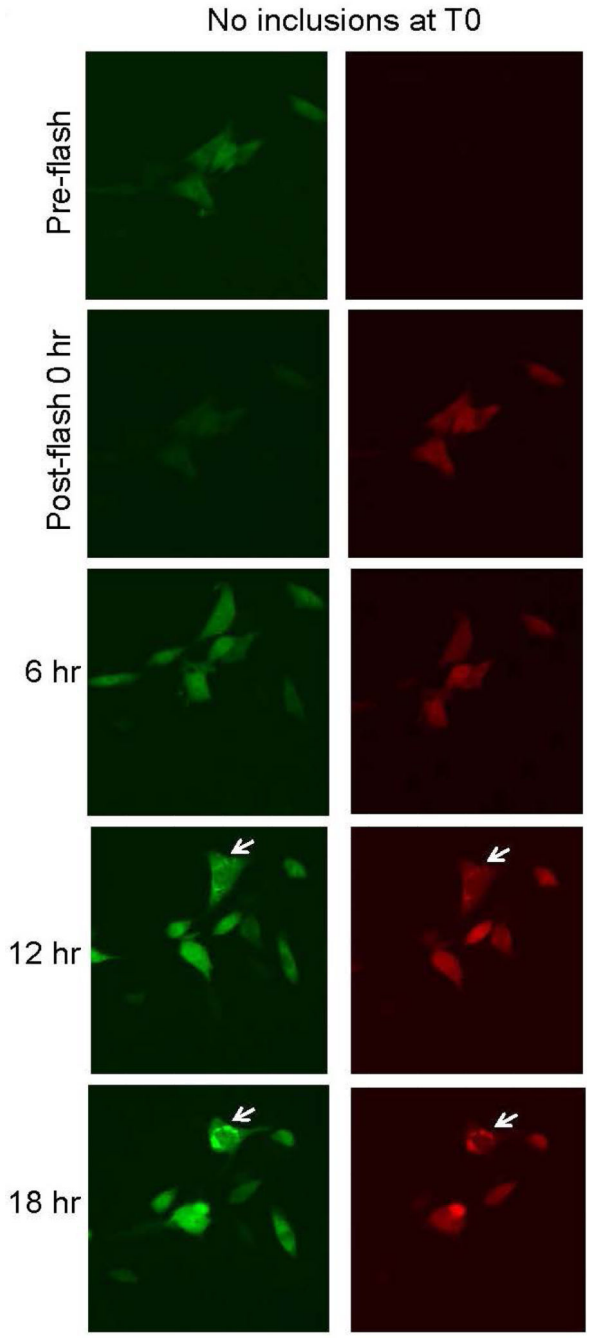

Fig. 2.

Images captured from time-lapse live imaging of CHO cells expressing A4V-SOD1:Dendra2 forming inclusions after 16 hours post-transfection. CHO cells were transiently transfected with expression plasmids for A4V-SOD1:Dendra2 and incubated for 16 hours before placement in an environmental chamber attached to a Nikon live-imaging microscope. Post-flash images are shown at time 0, 6, 12, and 18 hours.

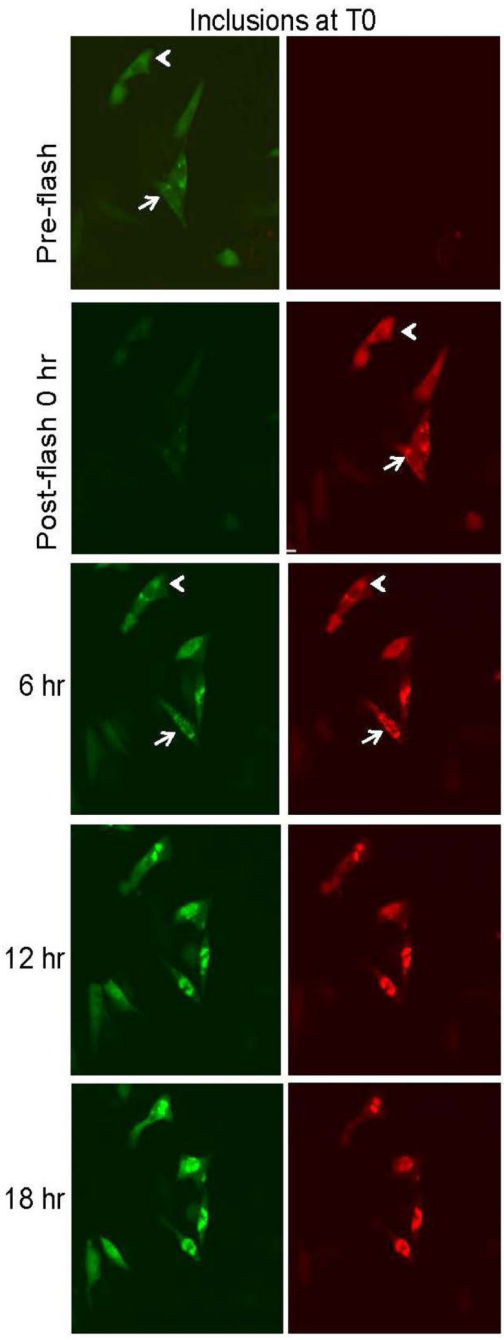

Fig. 3.

Images captured from time-lapse live imaging of CHO cells expressing A4V-SOD1:Dendra2 forming inclusion before 16 hours post-transfection. CHO cells were transiently transfected with expression plasmids for A4V-SOD1:Dendra2 and incubated for 16 hours before placement in an environmental chamber attached to a Nikon live-imaging microscope. Post-flash images are shown at time 0, 6, 12, and 18 hours.

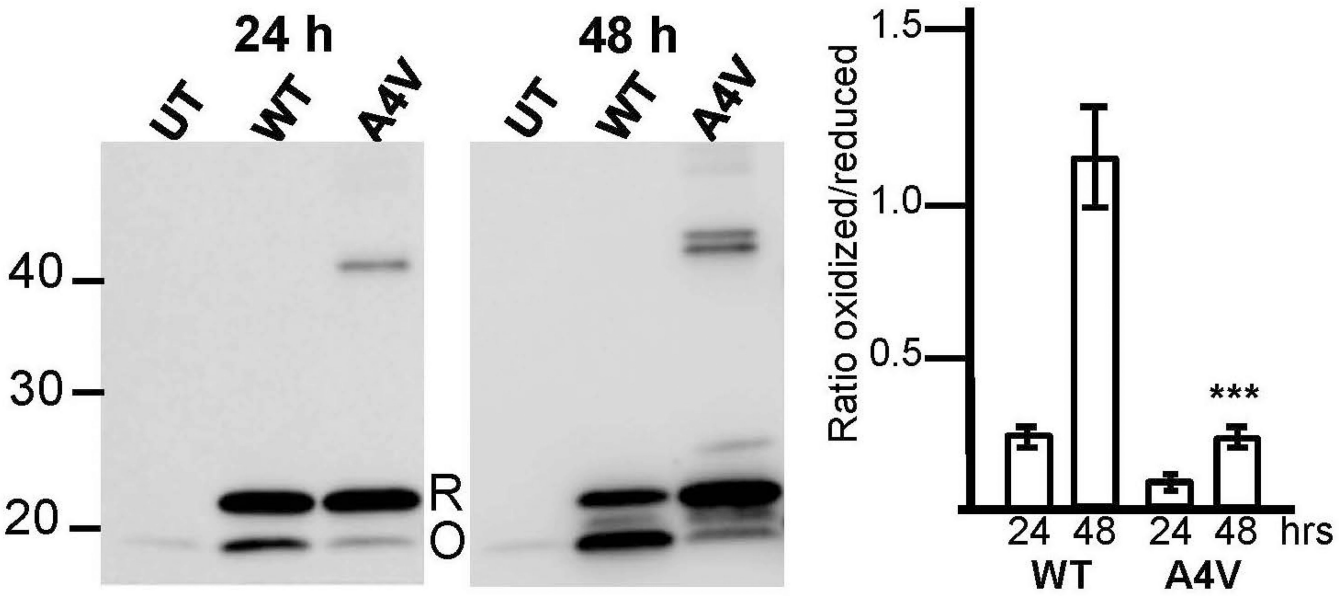

Fig. 4.

Variations in the formation of intramolecular disulfide bonds by soluble WT and A4V SOD1 extracted from HEK293FT cell. Following transfection in HEK293FT cells for either 24 or 48 hours, as indicated, with WT SOD1, mutant SOD1 constructs A4V, G85R, D101G, or D101N, or left untransfected (UT), cells were detergent extracted as described in "Experimental Procedures". 5μg of the detergent soluble fractions were analyzed by SDS-PAGE without reducing agent followed by an in-gel reduction in 2% β-mercaptoethanol. The ratio of oxidized (O) to reduced (R) SOD1 was quantified for each construct at both 24 and 48 hours [mean ratio ± S.E. (error bars) of three replicate experiments]. Analysis of variance (ANOVA) and Tukey's test were used to determine the statistical significance for mutant SOD1 oxidation at either 24 or 48 hours when compared to WT at the same timepoint: *** $P \leq 0.001$.

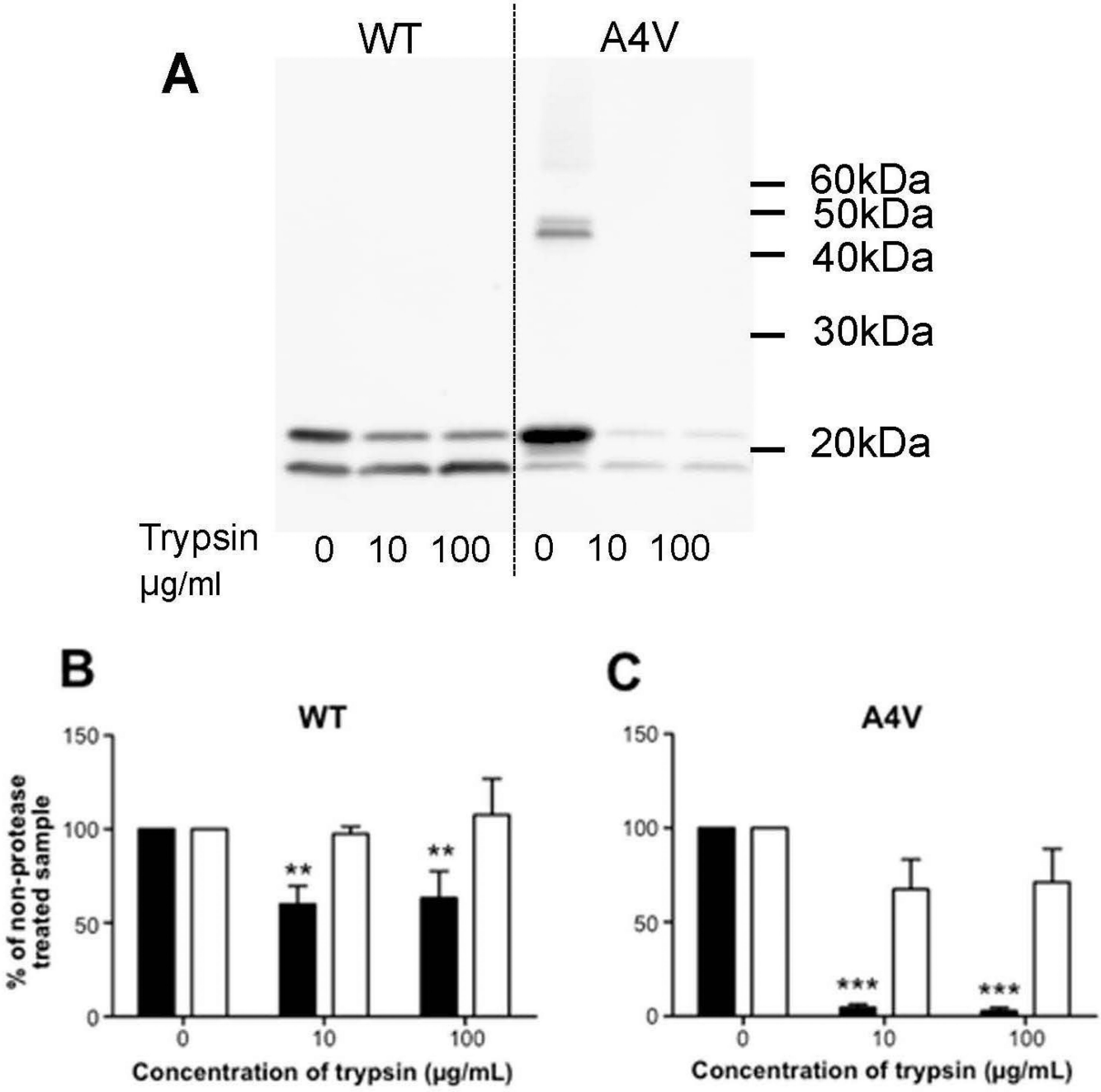

Fig. 5.

Sensitivity of the oxidized and reduced forms of NP-40 soluble SOD1 to proteolytic digestion. HEK293FT cells were transfected with the WT and A4V SOD1 constructs for 48 hours and detergent extracted as described in “Experimental Procedures”. *A*, 5µg of the NP-40 detergent soluble fractions were treated with various concentrations of trypsin and analyzed by SDS-PAGE without reducing agent followed by an in-gel reduction in 2% β-mercaptoethanol. The migration of the 20kDa band of the ladder is indicated on the left of the panel. *B-G*, the reduced (black bars) and oxidized (white bars) band intensities for each SOD1 construct were quantified in relation to the non-trypsin treated fraction [mean ratio ±

S.E. (error bars) of at least three replicate experiments]. ANOVA and Tukey's test was used to determine the statistical significance of the trypsin treated reduced or oxidized band intensities when compared to the non-treated samples: ** $P \leq 0.01$, *** $P \leq 0.001$.

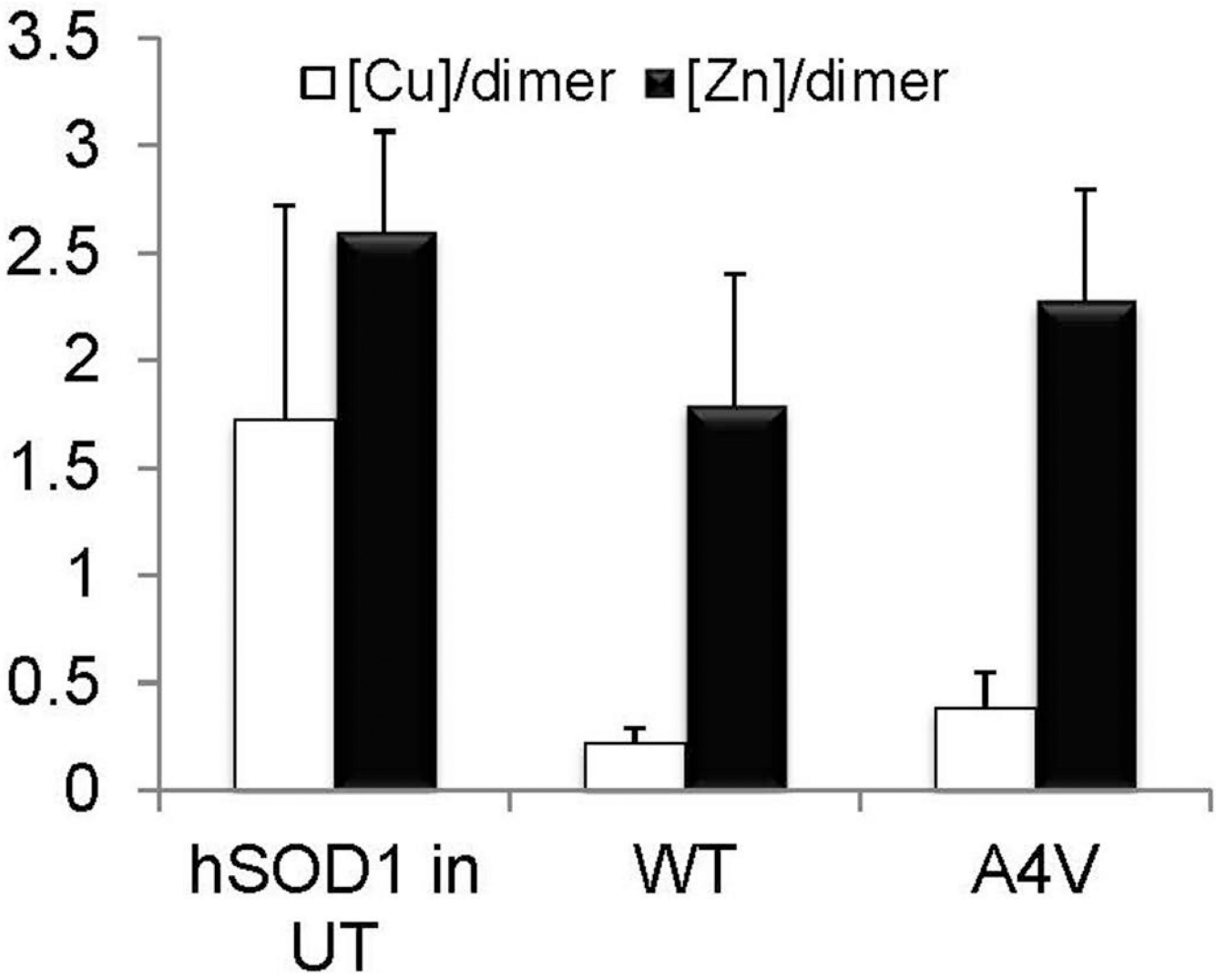

Fig. 6.

Metal content of soluble SOD1 isolated from HEK293FT cells expressing WT and mutant SOD1. The copper (Cu) and zinc (Zn) metallation state of soluble human SOD1 isolated from either untransfected HEK293FT cells or cells transfected for 24 hours with the SOD1 constructs listed were measured by HPLC-ICP-MS as described in “Experimental Methods”. The amount of Cu (black bars) and Zn (white bars) per dimer was calculated by dividing the metal concentration for each construct by its protein concentration [mean ratio ± S.E. (error bars) of at least three replicate experiments]. ANOVA and Tukey’s test was used to determine the statistical significance of the Cu and Zn levels for each of the mutants in comparison to the WT levels: ** $P \leq 0.01$, *** $P \leq 0.001$.

Table 1

Quantification of cells transiently transfected with A4V-SOD1:Dendra2

	Total red fluorescent cells at 0 hr	No. of cells with no inclusions at 0 hr and no inclusions at 18 hr	No. of cells with no inclusions at 0 hr that gained red inclusions by 18 hr / no. of those cells that also gained green inclusions [1]	No. of cells with red inclusions at 0 hr / no. of those cells that also gained green inclusions by 18 hr [2]
Trial 1	286	94	34/34	53/52
Trial 2	133	45	12/12	32/28
Trial 3	97	24	7/7	29/25

[1] Column represents cells depicted in Figure 1A

[2] Column represents cells depicted in Figure 1B